Macromolecules
ARTICLE

Macromolecules **2010**, *43*, 473–479 **473**
DOI: 10.1021/ma901624p

Construction of Continuous Porous Organogels, Hydrogels, and Bicontinuous Organo/Hydro Hybrid Gels from Bicontinuous Microemulsions

Shintaro Kawano, Daisuke Kobayashi, Shun Taguchi, and Masashi Kunitake*

New Frontier Sciences, Graduate School of Science and Technology, Kumamoto University, 2-39-1 Kurokami, Kumamoto, 860-8555, Japan

Taisei Nishimi

Frontier Core-Technology Laboratories, FUJIFILM Corporation, 210 Nakanuma, Minami-Ashigara, Kanagawa, 250-0193, Japan

Received August 9, 2009; Revised Manuscript Received October 13, 2009

ABSTRACT: A new class of unique soft gels was produced by gelations of bicontinuous microemulsions (BME). Three alternative composite gel systems, namely BME organogel, hydrogel and an organo/hydro hybrid gel, prepared by hydrogelation and/or organogelation of BME solutions were proposed. These gels were self-supported, and aqueous and oil microphases bicontinuously coexisted and were immobilized in the gels. Even in "one side only" gelation products such as the BME organogel and the BME hydrogel, alternate solvent phases without gelator were also macroscopically immobilized. Microscopic structures of the gels were confirmed by CLSM and SEM observation. The BME organogels or hydrogels and BME hybrid gels showed continuous porous structures and double network structures, respectively. Mesostructures of the gels significantly depended on gelation conditions. It was found that the hierarchical structure of the BME gels was regulated by competition among three synergetic rate factors: immobilization of the BME structure by gelation, mesoscopic phase separation by gelation, and the time-dependent transformation of a solution/solution structure toward a thermodynamic structure in an equilibrium state.

Introduction

A variety of unique, jelly like solid gels,[1] comprising three-dimensional polymeric networks containing solvents, have been intensively researched recently. These soft materials include stimuli-responsive (intelligent) gels,[2] double network gels,[3] nanocomposite gels[4] and topological gels.[5] Such gels are expected to have potential as polymer materials for actuators[2,6] and drug release systems,[2,7] which are key polymer technologies of the future. Soft "wet" gels have been categorized as organogels or hydrogels according to the solvent used; the solvent is the major component of the gels in terms of weight fraction. Generally, organogels and hydrogels have been prepared by gelation to form three-dimensional networks based on physical aggregation or chemical polymerization including cross-linking.

Gelation in emulsions or microemulsions, in which water and oil phases are microscopically separated and each phase is a macroscopically homogeneous solution, has been investigated as composite gel formation since the 1980s.[8] Hydrogel particles prepared by hydrogelation in W/O emulsion have been investigated.[9] Bulk organogels bearing water microdroplets prepared by organogelation in W/O emulsion have also been researched, because of medical applications such as dermal drug delivery.[10] As expected, the converse combinations are possible but have been rarely reported.[11]

The dynamic morphology of a microemulsion (ME) is generally determined by the hydrophilicity−lipophilicity balance (HLB) of the surfactants in the emulsion system. When the hydrophilicity and lipophilicity are well-balanced in the system, the microemulsion frequently possesses a bicontinuous structure, in which the water phase and the oil phase coexist on a microscopic scale, in a so-called bicontinuous microemulsion (BME) or "middle phase" microemulsion.[12] Recently, radical polymerization in a BME initiated by thermal,[13] redox,[14] and photo[15] initiators has received much attention in relation to formation of polymer blocks with a continuous porous structure, due to their potential as monolithic columns and ultrafiltration membranes. Very recently, Deen and co-workers reported the polymerization of a polymerizable surfactant in BME with various organic solvents.[16] Several organic solvents produced self-supported wet gels with a submicrometer scale structure based on BME solution even after polymerization. In this article, we report gelation of BME to produce three alternative composite gel systems, namely BME organogel, hydrogel, and organo/hydro hybrid gel, by hydrogelation and/or organogelation of BME solution. A BME organogel or a hydeogel were prepared by organogelation in micro organo phase or hydrogelation in micro aqueous solution phase in BME, respectively. A BME organo/hydro hybrid gel was constructed by double gelation with hydrogelation and organogelation in both micro phases of BME.

Experimental Section

Materials. Toluene (Nacalai. Co., Japan), Sodium dodecyl sulfate (SDS; Nacalai. Co., Japan), 2-butanol (Nacalai. Co., Japan), and NaCl (Wako Co., Japan) were used to prepare microemulsions without further purification. 12-Hydroxystearic acid (12HS; Tokyo Chemical Co., Japan), acrylamide (AAM; Kishida Chemical Co., Japan), *N*,*N*′-methylenebis(acrylamide) (MBAAM; Wako Co., Japan), ammonium peroxodisulfate

*Corresponding author. E-mail: kunitake@chem.kumamoto-u.ac.jp.

Published on Web 11/16/2009

(APS; Katayama Chemical Co., Japan), and *N,N,N′,N′*-tetramethylethylenediamine (TEMED; Wako Co., Japan) purchased were also used without further purification. 8-Hydroxypyrene-1,3,6-trisulfonic acid trisodium salt (HPTS, AnaSpec, Inc.; ex, 454 nm; em, 511 nm) and 4,4-difluoro-3,5-bis(4-phenyl-1,3-butadienyl)-4-bora-3a,4a-diaza-s-indacene (BODIPY 665/676, Invitrogen, Co. Ltd.; ex, 665 nm; em, 676 nm) as water-soluble and oil soluble, respectively, fluorescence dyes were used as received. Water ($R > 15$ MΩ) purified using a Milli-Q system (Millipore Co. Ltd.) was used to prepare aqueous solutions.

Preparation of BME Solution. Three-phase solutions with a middle (bicontinuous) phase were prepared according to the phase diagrams (Figure 1). The composition of the middle phase in a three-phase solution corresponds to the composition at the 4-fold point marked by arrow b. Because the presence of gelators and/or fluorescence dyes significantly changes the phase diagrams (see Figure S1), each recipe for BME solution was different and was moderated by concentrations of surfactant and cosurfactant. Typical recipes for three-phase microemulsions are shown in Table 1. On the phase diagram, the influence of the organo-gelator was relatively small and, the salt concentration was 20% increased in order to make an adjustment to deny the influence of gelator. The influence of a chemical hydro-gelator, AAM−MBAAM, was larger than that of organo-gelator. In order to deny the influence of AAM−MBAAM, the concentration of cosurfactant (2-buthanol) was increased by approximately 100%. The adding of 0.1 mM lipophilic dye did not influence the phase diagram at all. Besides, 10 mM hydrophilic dye had an obvious effect on the phase diagrams and whole concentration balance including surfactant had to be changed (See Table 1 and Figure S1).

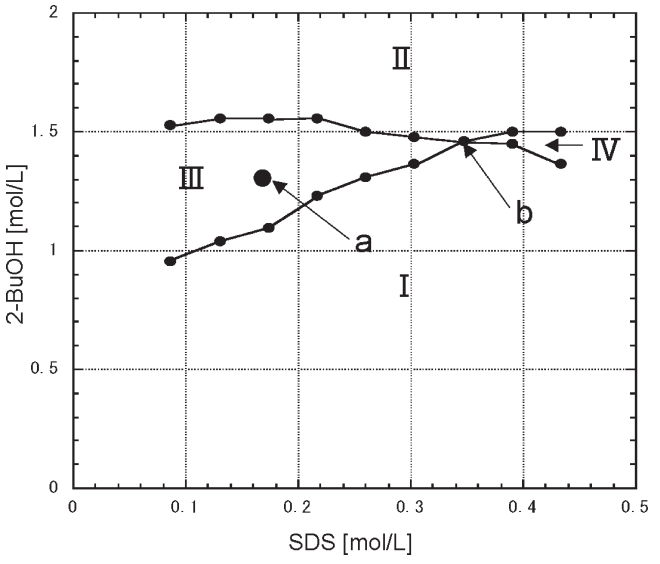

Figure 1. Typical phase diagram of a toluene/SDS+2-butanol/saline microemulsion comprising saline (1.1 M NaCl) and toluene at 25 °C. The regions I, II, III, and IV are attributed to O/W, W/O, three-phase solution including a middle phase (BME), and one phase type BME. The points marked by arrows a and b indicate the composition of A (Table 1) and the 4-fold point, respectively.

Gelation. BME organogels were prepared with 12-hydroxystearicacid (12HS, 30 mol % in toluene) as a lipophilic gelator. BME solution with 12HS was heated at 60 °C to dissolve the gelator and cooled to 5 °C with ca. 9 and 0.3 °C/min as rapid and slow gelation conditions, respectively (physical gelation). The typical gelation temperature of BME solutions (from "sol" to "gel") was determined by differential scanning calorimetry (DSC) as 9 °C.

Hydrogelation in BME was achieved by polymerization of AAM (30 wt % in water), MBAAM (19 mol % relative to AAM), and APS (1 mol % relative to monomer) with or without TEMED. Two different procedures, method A and method B, were conducted. In the case of method A, the two BME monomer solutions were prepared separately with the radical initiator ammonium persulfate (APS), and 1 mol % (relative to monomer) of the accelerator TEMED, respectively. Prior to the start of gelation, both solutions were allowed to stand for at least 1 h to reach equilibrium (stabilization time). After gentle mixing of the two BME solutions at room temperature, the mixture was heated at 60 °C to start polymerization which was complete in less than 10 min in the presence of the fluorescence dye. Method B is "rapid" gelation with 10 mol % TEMED without consideration of stabilization time. Gelation was started by directly adding and mixing TEMED with AAM−MBAAM BME "sol" in an ice bath at 0 °C: the reaction started instantly and gelation was completed in less than 15 min.

In order to prepare BME organo/hydro hybrid gel, a BME solution composed of 12HS (30 wt % in toluene) and AAM/MBAAM (in molar ratio 19/1) aqueous solution with APS (1 mol % relative to monomer) was prepared at room temperature. After 1 h stabilization at room temperature, polymerization was carried out for 1 h at 60 °C then the sample was cooled to 5 °C for physical gelation.

Characterization. Real space imaging of "wet" BME gels was performed by confocal laser scanning microscopy (CLSM; OLYMPUS, FV500-IX) using HPTS and BODIPY as water-soluble and oil soluble, respectively, fluorescence dyes. Typical concentrations of HPTS and BODIPY were 10 and 0.1 mM, respectively. The "wet" BME gel samples were frozen instantly in liquid nitrogen and dried by vacuum without change. The "dried" gel samples were broken to small pieces in liquid nitrogen. Prior to SEM observation (Tiny SEM of Technex Lab. Co. Ltd.), surfaces of the samples were coated with Au.

Results and Discussion

Macroscopic Observation of BME Organogel, Hydrogel, and Organo/Hydro Hybrid Gel. BME microemulsions were prepared as a middle phase in macroscopic three-phase solutions. The upper and lower phases were an oil phase and an aqueous phase, respectively (Figure 2a). The volume ratio of each three-phase solution was modified by adjusting the concentrations of salt and/or cosurfactant to make the solution with an equal volume of each phase, since the addition of gelator influenced the balance of the three phases. All of the BME solutions prepared were electroconductive due to

Table 1. Typical Composition of Each BME Solution Prepared for the BME Organogel, BME Hydrogel, and BME Organo/Hydro Hybrid Gel[a]

	BME solution					organogelation	hydrogelation			
	water (mL)	toluene (mL)	NaCl (mmol)	SDS (mmol)	2−BuOH (mmol)	12HS (mmol)	AAM (mmol)	MBAAM (mmol)	APS (mmol)	TEMED (mmol)
A	BME solution	5.0	5.0	5.0	1.7	12.9					
B	BME organogel	3.0	3.0	3.6 (3.0)	0.9	7.9	1.5				
C	BME hydrogel	3.0	3.0	3.0	0.9 (1.7)	13.2 (22.0)		7.6	0.56	0.24	0.11−1.1
D	BME organo/hydro hybrid gel	5.0	5.0	5.0	1.5 (2.6)	18.6 (28.0)	2.5	12.7	0.94	0.4	

[a] The values in parentheses show composition with fluorescence dyes

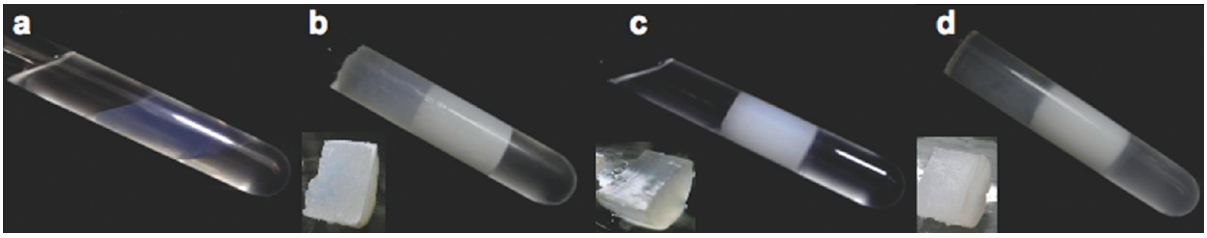

Figure 2. Photograph images of BME solution (a), BME organogel (b), BME hydrogel (c) and BME organo/hydro hybridgel (d) in three-phase solutions. Each inset photo shows a cross-sectional image of the BME gel taken out from the test tube and cut.

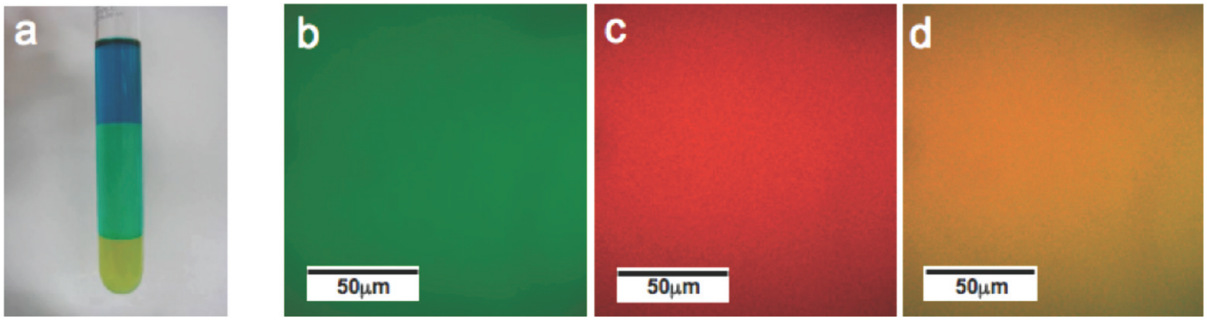

Figure 3. Photograph (a) of a typical three-phase ME solution with HPTS and BODIPY and CLSM images of homogeneous BME solution. HPTS image (b, aqueous microphase), BODIPY 665/676 (c, organic microphase) and superposition pattern of parts b and c (d).

continuous ionic migration of sodium and chloride ions in the aqueous phase.[17] In the case of "one side" organogelation (Figure 2b), the upper oil phase and middle phase were immobilized, but the bottom aqueous phase was not immobilized. In the case of "one side" hydrogelation (Figure 2c), the upper oil phase was not immobilized and the middle phase and lower aqueous phase were immobilized. In "both sides" gelation (Figure 2d), all three phases were gelled. The BME organogel and BME hybrid gel located at the middle phase were opaque but the BME hydrogel was translucent, though the BME solutions before gelation were almost transparent. It should be noted that a higher concentration of gelator was required to immobilize BME solutions than for homogeneous media (either organogelation or hydrogelation).

When the BME gels were taken out of the test tubes, they were connected to translucent hydrogel from the lower layer or/and translucent organogel from the upper layer. The BME gels were self-supporting, and very soft and elastic. No macroscopic pores were observed for all three types of BME gels on cutting the cross sections shown in the insets to Figure 2. Moreover, all BME gels revealed ionic conductivity, proving that the aqueous phase was continuous and the bicontinuous structure was retained in the composite gels. Interestingly, even in "one side only" gelation products such as the BME organogel and the BME hydrogel, alternate solvent phases without gelator were also macroscopically immobilized, although a very small amount of solvent oozed from the gels when they were compressed.

In addition, the gelation of uniform BME solution without excess saline and oil macrophases which is attributed to the 4-fold point (the mark b in Figure 1) was also conducted and gave essentially the same gelation products as those formed in a three-phase solution.

Microscopic Observation of BME Organogel. To observe "wet gel" structures without drying, CLSM observation of BME gels was conducted with hydrophilic (HPTS) and lipophilic (BODIPY) respectively, fluorescence dyes. Because of three-dimensional mapping at submicrometer scale by the discrimination between saline phase and oil phase, CLSM is a nondestructive powerful monitoring tool in characterizing the bicontinuous microemulsions. In a pioneer work, the elucidation of the three-dimensional network structures of "wet" polymer gels by CLSM observation was reported by Jinnai.[18]

In order to confirm the potential of CLSM and dyes used, a BME solution with dyes was observed by CLSM prior to the observation of BME gels. Figure 3a shows photographs of a three phase BME solution with fluorescence dyes and no gelator. Three phases, toluene phase, aqueous phase and middle phase were clearly represented as blue, green, and mixed colors. The fluorescence images of the homogeneous BME solution (middle phase) from HPTS and BODIPY and the superposition image (HPTS/BODIPY) are shown in Figure 3b−d, respectively. These results clearly proved that the oil phase and the aqueous phase were microscopically mixed entirely in the middle phase. The aqueous region, oil region and well-mixed region on a submicrometer scale can be discriminated as green, red, and yellow colors. However, the texture of the original BME solution was not confirmed due to the resolution limit of CLSM.

Whereas the thickness (or volume) of oil and aqueous liquid layers in a microemulsion is thermodynamically controlled by the hydrophilicity and lipophilicity of the surfactant system, the structure of BME gels is strongly influenced by the kinetics of the gelation process. Kinetic control of the physical gelation process to produce BME organogels was relatively simply achieved by control of the rate of cooling from the "sol state" to the "gel state". Figure 4 shows typical CLSM images of two BME organogels formed at different gelation speeds. The BME organogel prepared by "rapid gelation" cooling from 60 to 5 °C at ca. 9 °C min^{-1} (Figure 4a) gave a texture-less yellowish CLSM image. The image was very similar to those of a "sol" state or homogeneous BME solution without gelator, even though the CLSM image of BME organogels revealed an unclear bleary feature by comparison with that of a BME solution (see Figure 3d). The yellowish color indicates that both oil and saline phases were uniformly mixed on a submicrometer scale. The CLSM images clearly proved that "rapid gelation" possibly achieved immobilization of the solution structure in BME less than several hundred nm.

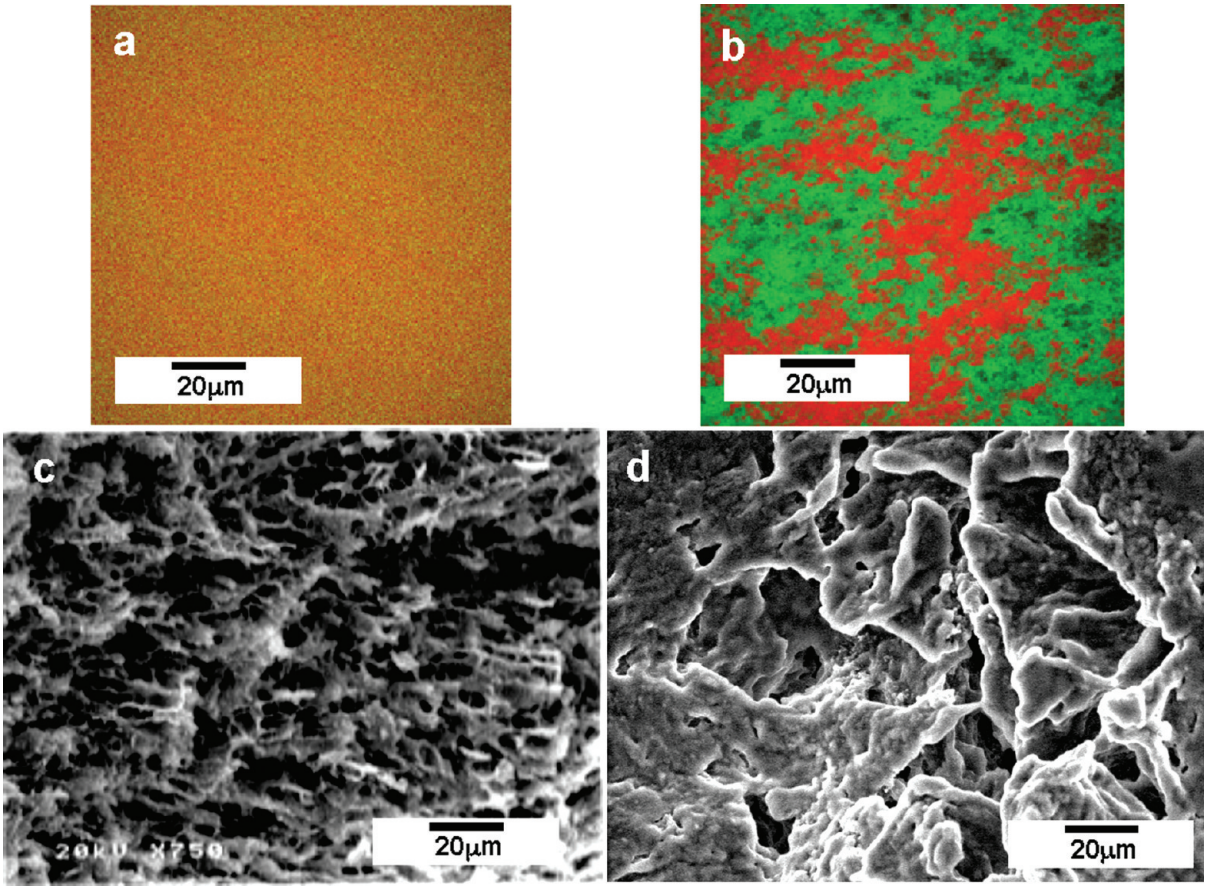

Figure 4. Typical CLSM (a,b) and SEM (c,d) images of BME organogel prepared by " rapid" cooling with the rate of 9 °C/min (a) and " slow " cooling with 0.3°C/min (b).

In contrast, the BME organogel prepared by "slow" gelation cooling at ca. 0.3 °C min^{-1} from 60 to 5 °C revealed a mosaic pattern of two large domains discriminated by green and red colors, indicating mesoscopic phase separation as shown in Figure 4b. The "green" aqueous regions and "red" oil regions were separated bicontinuously on a scale of several tens of micrometers, and no yellowish region was observed.

The driving force of mesoscopic phase separation is the lowering of the surfactant activity by gelation. As noted above, the thickness of the liquid layers in BME is determined thermodynamically by the hydrophilicity and lipophilicity of the surfactant system, and each liquid layer thickness is increased in BME with increasing hydrophilicity or lipophilicity. In addition, the propagation of gel fibers in oil or aqueous microphases kinetically induces lowering of the surfactant activity following mesoscopic phase separation, in which aqueous and oil phases progressively separate.[19] The mesoscopic phase separation mechanism is similar to that of spinodal decomposition from the viewpoint of kinetic control. Since immobilization of a bicontinuous solution structure and mesoscopic phase separation proceed competitively during gelation, the structures of the BME gels were modulated kinetically as a function of gelation speed. Similarly, mesoscopic phase separation induced by polymer propagation was observed in the case of polymerization of styrene-based BME (see Figure S2).

Even in the "rapid" condition we conducted, the microstructure might be influenced by mesoscopic phase separation. Because of the limit of resolution and dynamics, the thickness of BME solution before gelation cannot be estimated at a range less than 100 nm by CLSM. The estimation of solution thickness of BME has been done using the small angle neutron scattering method (SANS),[20] the transmission electron microscope (TEM) with freeze−fracture replica technique,[21,22] and a simulation.[23] The thicknesses reported were estimated in the range between several tens of nanometers and 100 nm and depended on the emulsion systems and the measurement method. As a direct visual estimation, TEM observation of a freeze−fracture replica sample has been reported. Abe and co-workers have observed typical textures with a range less than 100 nm for polymeric silicone BME systems.[21]

Parts c and d of Figure 4 show typical SEM images of freeze-dried samples of the BME organogel. Prior to SEM observation, the gel samples were frozen and crushed in liquid nitrogen to minimize the influence of drying. An SEM image of the BME organogel prepared by rapid cooling (Figure 4c) revealed a uniform sponge-like porous structure. The wall of the porous structure consisted of organogel fiber networks. The regular pore size of the BME organogel obtained from SEM images was approximately 5 μm. The sizes were ten times larger than the maximum size (0.1 μm) expected from the featureless CLSM image (Figure 4a) of the "wet" BME organogel prepared under the same conditions. The difference between the "wet" CLSM image and the "dry" SEM image indicates that the sponge-like structure with larger pores was created by drying, even though the SEM sample was prepared by freeze-drying to minimize such an influence. In a control experiment, the SEM image of a homogeneous toluene gel with 12HS prepared under similar conditions revealed a pore-free surface (see Figure S3). It follows that the continuous porous structure observed in the

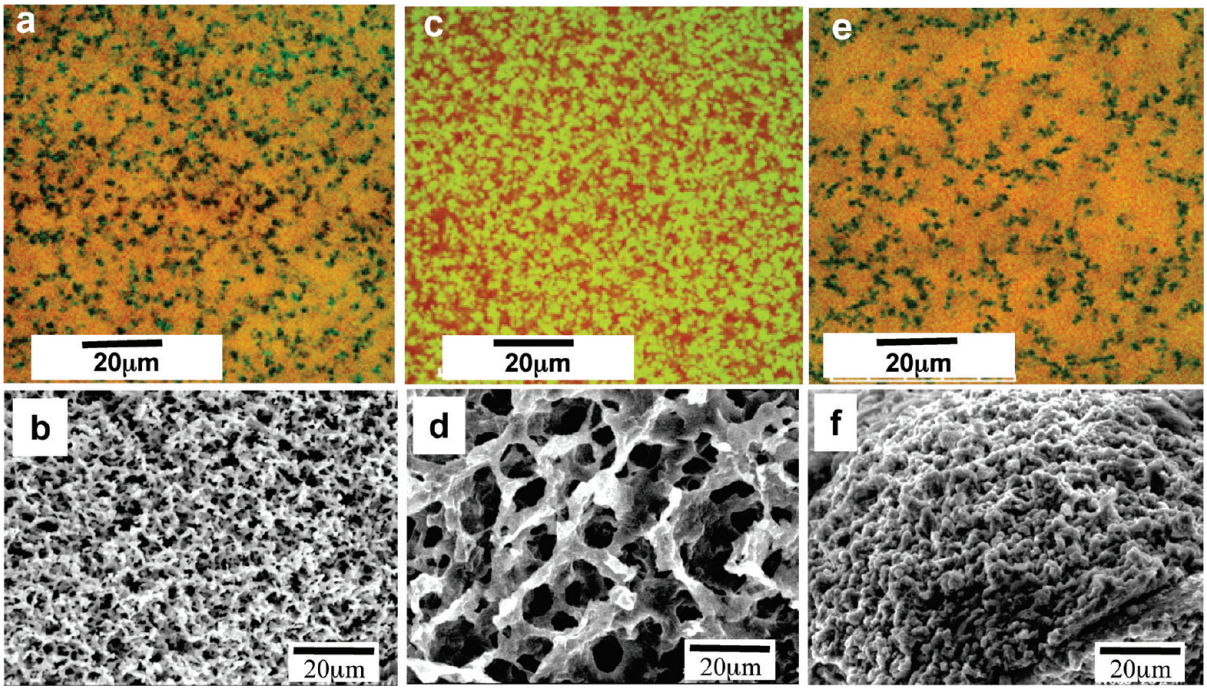

Figure 5. CLSM (a, c, and e) and SEM (b, d, and f) images of the BME hydrogel (a−d) and BME organo/hydro hybridgel (e and f). The BME hydrogels were prepared by method A (a and b) and method B (c and d). Concentrations of TEMED (for monomer) are nothing (e and f), lmol % (a and b) and 10 mol % (c and d).

SEM image originated from the aqueous region in BME, confirming the formation of a bicontinuous structure in the BME gel. The SEM image of the BME gel sample, corresponding to Figure 4b, prepared by "slow" organogelation (Figure 4d), shows larger canyons and no micropores.

Microscopic Observation of BME Hydrogel. Similar to BME organogels prepared by physical gelation, chemical hydrogelation in BME allowed us to produce bicontinuous composite gels consisting of an oil microphase and a hydrogel microphase, with various meso-structures regulated generally by gelation speed. It is well-known that addition of TEMED accelerates polymerization of AAM−MBAAM monomer. When TEMED (typically 1 mol % relative to monomer) was added to a BME gelation system in the absence of the fluorescence dyes, gelation was completed within 1 min even at temperatures below room temperature. The presence of the hydrophilic fluorescence dye prohibited acceleration by TEMED. In the case of BME solution in the presence of the fluorescence dyes, a high concentration of TEMED (typically 10 mol %) was necessary for rapid hydrogelation to occur within several minutes.

It is worth recalling that a microemulsion system needs time to reach thermodynamic equilibrium. Even when the solution seems to be macroscopically homogeneous, the thickness of the liquid layer for the bicontinuous phase may be changed continuously toward an equilibrium state after mixing. When macroscopic three-phase solutions were shaken, a mixed solution separated instantaneously into three phases, but the volume ratio of the three phases changed in the time required to reach equilibrium. The volume of the bicontinuous middle phase gradually decreased as extra water and oil were pushed out. Consequently, the stabilization time required to reach equilibrium after preparing the BME solution and before gelation was also an important parameter for controlling the microstructures of the BME gels.

In fact, the stabilization time and use of a polymerization accelerator have a trade-off relationship, because immobilization of BME solution starts immediately on addition of TEMED to a BME solution before the emulsion system can reach thermodynamic equilibrium. With increased concentration of TEMED, the immobilization speed is increased but the time required to reach the most stable bicontinuous structure with minimum layer thickness is reduced. In contrast, the BME hydrogel system without TEMED had a relatively long stabilization time at room temperature prior to polymerization at high temperature.

Typical CLSM images and SEM images of two BME hydrogels prepared in two typical different conditions (methods A and B) are shown in Figure 5a−d. In the CLSM image (Figure 5a) of BME hydrogel formed under method A conditions, a yellowish featureless texture coexists with green (black) islands with micrometer scale. The yellowish region is attributed to ideally immobilized BME hydrogel on a submicrometer scale. The green (black) colored islands are aqueous regions separated from BME. The black region is the hydrophilic area with discolored hydrophilic dye. Consequently, the formation of green islands was caused by mesophase separation, due to pushing out excess water from a bicontinuous microphase. The contraction of the aqueous microphase is due to reduction of the hydrophilicity of the surfactant system by hydrogelation. In addition, a bulk AAM−MBAAM hydrogel gave a homogeneous CLSM image and no such meso-separation was observed (see Figure S3).

A similar morphology to that of composite BME solution, consisting of a yellowish featureless texture and green islands, was observed for the BME hydrogel system prepared by polymerization without an accelerator at 60 °C, with sufficient stabilization time (several hours) at room temperature. The average size of the dark green islands was roughly twice the size of those prepared by method A with the accelerator, indicating that phase separation to form micro hydrogel islands from BME gels was minimized by kinetically facilitated gelation with TEMED.

Parts c and d of Figure 5show CLSM and SEM images, respectively, of the BME hydrogel prepared by "rapid" gelation with 10 mol % TEMED without consideration of

stabilization time (method B). The reaction started instantly and gelation was completed in less than 15 min. Interestingly, it was found that a homogeneous bicontinuous structure formed, consisting of the micrometer scale isolated green and red regions shown in Figure 5c. There was almost no yellowish region and the green and red regions did not overlap on the CLSM scale. The size of the bicontinuous texture with scale between submicrometer and several ten of micrometers was able to be controlled by reaction temperature.

The SEM images (Figure 5, parts b and d) of "freeze dried" samples of both BME hydrogels (methods A and B) showed similar continuous porous network structures. The structures of the dried samples observed were direct proof of the bicontinuous structure of BME hydrogels in the "wet" state, because the simple hydrogel (AAM/MBAAM) had a pore-free network structure (see Figure S3). From method A, a continuous porous network structure with 1−5 μm pores was observed for the dried sample prepared from the gel. Although a yellowish featureless textured region and green island region were clearly recognized in the CLSM image (Figure 5a), no such separated region could be seen in the SEM image of the corresponding dried sample.

The SEM image (Figure 5d) of the BME hydrogel prepared by method B, in which mesoscopic phase separation on a ca. 5 μm scale was observed, showed a similar continuous network structure with larger pores (5−20 μm). Interestingly, the continuous porous network structures formed by method B resembled the structures produced by method A, notwithstanding the different scale of the pore size. A similar physical appearance of continuous porous structure has also been reported for monolithic silica prepared by spinodal decomposition based on the sol−gel method. Nakanishi et al.[24] have reported the construction of monolithic silica columns and their application as column packing materials for high performance liquid chromatography (HPLC). The morphologies of the porous materials, especially pore size, are controlled by the reaction kinetics and reaction parameters such as chemical structure and concentration of silica precursor, external solvents and temperature. It is noteworthy that both techniques can produce very similar continuous porous structures, despite entirely different approaches and materials. Very recently, Jinnai and co-workers have reported porous NIPAAm polymer gel prepared by spinodal decomposition.[18,25]

Microscopic Observation of BME Organo/Hydro Hybrid Gel. Figures 5e and f show typical CLSM and SEM images for the BME hybrid gels made by double gelation in both oil and saline microphases. Gong and co-workers reported double network (DN) hydrogel systems that were very tough and showed low friction, and discussed the resemblance of the DN gels to biosystems.[3] Prior to heating for chemical gelation, the BME solution in the presence of 12HS and AAM/MBAAM without TEMED was prepared at room temperature and allowed to stand for 1 h. Then polymerization was conducted at 60 °C, and the sample was cooled to 5 °C for physical gelation.

The structure of the BME hybrid gel consisted of the homogeneous BME gel phase (yellowish) and separated islands (green) shown in Figure 5e. The texture in the CLSM image was very similar to that of the BME hydrogel prepared by method A. Formation of separated islands of hydrogel microphase was induced by hydrogelation but not by organogelation. As hydrogelation was conducted prior to organogelation, the mesostructure of the hybrid gels was determined by the chemical gelation step.

Compared with the porous network structures of "one side" gelled samples, the morphology of BME hydrogel observed by SEM was entirely different despite the resemblance of the CLSM images. Figure 5f shows that the SEM image of the BME hybrid gel had a pore-free smooth surface. These results clearly proved the existence of a hybrid gel system in which the both organic and aqueous microphases were immobilized by each gelation step.

Conclusions

The novel methodology we proposed, the gelation of BME, allows us to provide various unique hybrid "wet" gel products consisted of water microphase and oil microphase. Continuous porous structures were produced by alternate gelation of organo phase or aqueous phase in a BME. Moreover, bicontinuous organo/hydro hybrid gel are provided by gelation of the both phase. The hierarchical structure of the BME gels was regulated by competition of three synergetic rate factors, namely immobilization of BME structure by gelation, mesoscopic phase separation by gelation, and the time-dependent transformation of solution/solution structure toward thermodynamic structure in equilibrium state. These results should lead us to the development of promising novel composite soft materials with hierachiral nanostructures prepared by various combinations of polymerization and/or gelation in BME in the future. Detailed studies including physical properties are in progress.

Acknowledgment. This work was supported by CREST (Core Research for Evolutional Science and Technology) of JST (Japan Science and Technology Corporation) and a Grant-in Aid for Scientific Research from the Ministry of Education, Science, Sports, and Culture.

Supporting Information Available: Figures showing the phase diagram of a toluene/SDS + 2-butanol/saline microemulsion, various SEM images of continuous porous polystyrene products, and CLSM and SEM images. This material is available free of charge via the Internet at http://pubs.acs.org.

References and Notes

(1) Osada, Y.; Khokhlov, A. R. *Polymer Gels and Networks*; CRC Press: New York, 2001.
(2) (a) Osada, Y.; Okuzaki, H.; Hori, H. *Nature* **1992**, *355*, 242. (b) Holtz1, J. H.; Asher, S. A. *Nature* **1997**, *389*, 829. (c) Siegel, R. A. *Nature* **1998**, *394*, 427. (d) Yoshida, R.; Sakai, K.; Okano, T.; Sakurai, Y. *J. Biomater. Sci., Polym. Ed.* **1994**, *6*, 585. (e) Hirose, M.; Kwon, O. H.; Yamato, M.; Kikuchi, A.; Okano, T. *Biomacromolecules* **2000**, *1*, 377.
(3) (a) Yang, W.; Furukawa, H.; Gong, J. P. *Adv. Mater.* **2008**, *20*, 4499. (b) Gong, J. P.; Katsuyama, Y.; Kurokawa, T.; Osada, Y. *Adv. Mater.* **2003**, *15*, 1155.
(4) Haraguchi, K.; Takehisa, T. *Adv. Mater.* **2002**, *14*, 1120.
(5) (a) Sakai, T.; Murayama, H.; Nagano, S.; Takeoka, Y.; Kidowaki, M.; Ito, K.; Seki, T. *Adv. Mater.* **2007**, *19*, 2023. (b) Okumura, Y.; Ito, K. *Adv. Mater.* **2001**, *13*, 485.
(6) Fukushima, T.; Asaka, K.; Kosaka, A.; Aida, T. *Angew. Chem., Int. Ed.* **2005**, *44*, 2410.
(7) Sakata, S.; Uchida, K.; Kaetsu, I.; Kita, Y. *Radiat. Phys. Chem.* **2007**, *76*, 733.
(8) Rees, D. G.; Robinson, H. B. *Adv. Mater.* **1993**, *5*, 608.
(9) (a) Hernandezbarajas, J.; Hunkeler, D. J. *Polym. Adv. Technol.* **1995**, *6*, 509. (b) Dowding, P. J.; Vincent, B.; Williams, E. *J. Colloid Interface Sci.* **2000**, *221*, 268.
(10) (a) Trickett, K.; Eastoe, J. *Adv. Colloid Interface Sci.* **2008**, *144*, 66. (b) Jadhav, R. K.; Kadam, J. V.; Pisal, S. S. *Current Drug Delivery* **2009**, *6*, 174. (c) Murdan, S. *Expert Opin. Drug Delivery* **2005**, *2*, 489.
(11) (a) Chen, H.; Chang, X.; Du, D.; Li, J.; Xu, H.; Yang, X. *Int. J. Pharm.* **2006**, *315*, 52. (b) Kreilgaard, M. *Pharm. Res.* **2001**, *18*, 367.
(12) (a) Shinoda, K.; Arai, H. *J. Phys. Chem.* **1964**, *68*, 3485. (b) Saito, H.; Shinoda, K. *J. Colloid Interface Sci.* **1970**, *32*, 647. (c) Shinoda, K.; Kunieda, H. *J. Colloid Interface Sci.* **1973**, *42*, 381. (d) Guering, P.; Lindman, B. *Langmuir* **1985**, *1*, 464.
(13) (a) Antonietti, M.; Hentze, H. P. *Colloid Polym. Sci.* **1996**, *274*, 696. (b) Hao, J. *J. Polym. Sci., Part A: Polym. Chem.* **2001**, *39*, 3320.

(c) Cameron, N. R.; Flook, K. J.; Wren, S. A. C. *Chromatographia* **2003**, *57*, 203.
(14) (a) Li, T. D.; Gan, L. M.; Chew, C. H.; Teo, W. K.; Gan, L. H. *J. Membr. Sci.* **1997**, *133*, 77. (b) Liu, J.; Gan, L. M.; Chew, C. H.; Teo, W. K.; Gan, L. H. *Langmuir* **1997**, *13*, 6421.
(15) (a) Peinado, C.; Bosch, P.; Martin, V.; Corrales, T. *J. Polym. Sci., Part A: Polym. Chem.* **2006**, *44*, 5291. (b) Deen, G. R.; Gan, L. H.; Gan, Y. Y. *Polymer* **2004**, *45*, 5483.
(16) Deen, G. R.; Gan, L. H. *J. Polym. Sci., Part A: Polym. Chem.* **2009**, *47*, 2059.
(17) (a) Yoshitake, S.; Ohira, A.; Tominaga, M.; Nishimi, T.; Sakata, M.; Hirayama, C.; Kunitake, M. *Chem. Lett.* **2002**, *31*, 360. (b) Kunitake, M.; Murasaki, S.; Yoshitake, S.; Ohira, A.; Taniguchi, I.; Sakata, M.; Nishimi, T. *Chem. Lett.* **2005**, *34*, 1338.
(18) Hirokawa, Y.; Okamoto, T.; Kimishima, K.; Jinnai, H.; Koizumi, S.; Aizawa, K.; Hashimoto, T. *Macromolecules* **2008**, *41*, 8210.
(19) *Advances in Polymer Science*; Springer: Berlin and Heidelberg, Germany, 2004.
(20) Ryan, L. D.; Kaler, E. W. *J. Phys. Chem. B* **1998**, *102*, 7549.
(21) Sharma, S. C.; Tsuchiya, K.; Sakai, K.; Sakai, H.; Abe, M.; Miyahara, R. *J. Oleo Sci.* **2008**, *57*, 669.
(22) Ikeda, Y.; Imae, T.; Hao, J.; Iida, M.; Kitano, T.; Hisamatsu, N. *Langmuir* **2000**, *16*, 7618.
(23) Nagarajan, R.; Ruckenstein, E. *Langmuir* **2000**, *16*, 6400.
(24) Nakanishi, K. *J. Porous Mater.* **1997**, *4*, 67.
(25) Hirokawa, Y.; Jinnai, H.; Nishikawa, Y.; Okamoto, T.; Hashimoto, T. *Macromolecules* **1999**, *32*, 7093.